MULTISCALE MODEL. SIMUL.
Vol. 15, No. 4, pp. 1448–1471

CARBON-NANOTUBE GEOMETRIES AS OPTIMAL CONFIGURATIONS*

E. MAININI†, H. MURAKAWA‡, P. PIOVANO§, AND U. STEFANELLI¶

Abstract. The fine geometry of carbon nanotubes is investigated from the viewpoint of molecular mechanics. Actual nanotube configurations are characterized as locally minimizers of a given configurational energy, including both two- and three-body contributions. By focusing on so-called zigzag and armchair topologies, we prove that the configurational energy is strictly minimized within specific, one-parameter families of periodic configurations. Such optimal configurations are checked to be stable with respect to a large class of small nonperiodic perturbations and do not coincide with classical *rolled-up* nor *polyhedral* geometries.

Key words. carbon nanotubes, configurational energy, stability

AMS subject classification. 82D25

DOI. 10.1137/16M1087862

1. Introduction.

Carbon nanotubes are allotropes of carbon consisting of long, cylindrical, hollow structures including as many as 10^7 atoms [44]. These are covalently bonded, thus sharing a pair of electrons. The corresponding orbitals are so-called sp^2-hybridized, inducing indeed bonds at a given atom to form $2\pi/3$ angles, as happens in *alkenes* [4]. As a result, the local topology of atomic bonds is hexagonal, for each atom has exactly three active bonds, approximately forming $2\pi/3$ angles. Although evidence of carbon filaments has to be traced back at least to the 1950s [34], a new branch of carbon-nanotube chemistry definitely emerged from the early 1990s with [21] and [2, 22]; see the review [32]. Since then, carbon nanotubes have been subject of intensive investigation under a variety of different experimental and computational techniques [24, 20].

The unique trait of carbon nanotubes is their amazing aspect-ratio: structures of a few nanometers in diameter can have lengths up to several centimeters, thus bridging molecular and macroscopic scales. In addition, carbon nanotubes show remarkable mechanical strength [26, 43, 46] and, depending on the topology, high elec-

*Received by the editors August 3, 2016; accepted for publication (in revised form) August 1, 2017; published electronically October 24, 2017.
http://www.siam.org/journals/mms/15-4/M108786.html
Funding: The first author's work was supported by the Austrian Science Fund (FWF) project M 1733-N20. The second author's work was supported by JSPS KAKENHI grant 17K05368. The third author's work was supported by the Austrian Science Fund (FWF) project P 29681 and from the Vienna Science and Technology Fund (WWTF), the City of Vienna, and Berndorf Privatstiftung through Project MA16-005. The fourth author's work was supported by the Austrian Science Fund (FWF) projects P 27052, I 2375, and F 65 and from the Vienna Science and Technology Fund (WWTF) through Project MA14-009.
†Dipartimento di Ingegneria meccanica, energetica, gestionale e dei trasporti (DIME), Università degli Studi di Genova, via all'Opera Pia 15, 16145 Genova, Italy (edoardo.mainini@unipv.it).
‡Faculty of Mathematics, Kyushu University, 744 Motooka, Nishiku, Fukuoka, 819-0395, Japan (murakawa@math.kyushu-u.ac.jp).
§Faculty of Mathematics, University of Vienna, Oskar-Morgenstern-Platz 1, A-1090 Vienna, Austria (paolo.piovano@univie.ac.at).
¶Faculty of Mathematics, University of Vienna, Oskar-Morgenstern-Platz 1, A-1090 Vienna, Austria and Istituto di Matematica Applicata e Tecnologie Informatiche "E. Magenes", CNR, v. Ferrata 1, I-27100 Pavia, Italy (ulisse.stefanelli@univie.ac.at).

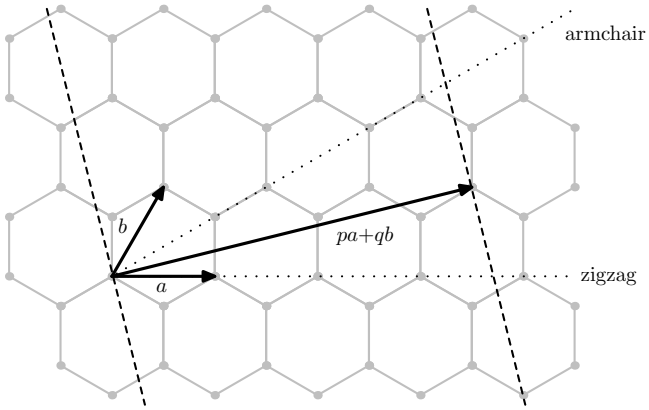

FIG. 1. *The identification $x \mapsto x + \ell a + mb$ on the hexagonal lattice defines the topology of the atomic bonds of the nanotube.*

trical conductivity or semiconductivity [25, 33]. Such exceptional properties make carbon nanotubes interesting for the development of innovative technologies. Carbon nanotubes are presently used in the production of composite materials, coatings, microelectronics, energy-storage devices, and biotechnologies [8].

Carbon nanotubes can be intuitively visualized as the result of the rolling-up of graphene, a two-dimensional carbon sheet where atomic bonds form an ideal hexagonal pattern. More precisely, let the *hexagonal lattice* $\mathcal{H} := \{pa+qb+rc : p, q \in \mathbb{Z},\ r = 0, 1\}$ with $a = (\sqrt{3}, 0)$, $b = (\sqrt{3}/2, 3/2)$, and $c = (\sqrt{3}, 1)$ represent graphene. We may prescribe the topology of the atomic bonds of a nanotube by specifying a vector (ℓ, m) for ℓ, $m \in \mathbb{N}$, $\ell > 2$ and identifying $x \in \mathcal{H}$ with $x + \ell a + mb$; see Figure 1. This identification actually defines the roll-up, an example of a resulting structure being in Figure 5. Nanotubes are called *zigzag* for $m = 0$, *armchair* for $m = \ell$, and *chiral* in all other cases. We concentrate here on zigzag and armchair topologies, leaving the chiral case aside, for it involves additional intricacies.

The fine geometry of carbon nanotubes is presently still debated, and different models are available. In the zigzag and armchair case, the classical *rolled-up* [9, 10] model is directly inspired by the above idealized identification and assumes that two of the three bond angles at each atom are exactly $2\pi/3$. An alternative is the *polyhedral* model [6, 7], which prescribes the three bond angles at each atom to be equal; see also the generalization in [27].

All the mentioned nanotube models are *geometrical* in nature for they reside on sets of geometrical postulates. The aim of this note is instead to follow a *variational* approach by investigating carbon-nanotube geometries within the frame of molecular mechanics [1, 28, 35]. Atom configurations are modeled as a collection of particle positions, to which a *configurational energy* is associated. This energy is given in terms of classical potentials and takes into account both attractive-repulsive *two-body* interactions, minimized at some given bond length, and *three-body* terms favoring $2\pi/3$ angles between bonds [41, 42]. This simplified, phenomenological approach is obviously very far from the quantum-mechanical nature of actual chemical bonding. Still, it has the advantage of being simple and parametrizable and of delivering the only computationally amenable option as the dimension of the ensemble scales up, as with the case of carbon nanotubes.

We single out specific carbon-nanotube geometries by focusing on their *stability*. This concept is central with respect to the process of molecular structuring, since among the many theoretically possible geometries, only those showing some suitable stability can be expected to be realized. This is formalized here by interpreting stability as the minimality of the configurational energy with respect to small perturbations. This approach is fairly classical, at least in the case of infinite crystals, where a number of different stability criteria has been set forth, essentially by prescribing specific set of admissible perturbations [14, 15]. The reader is referred to the discrete-to-continuous analysis in [12, 13] and the recent comparison in [36] of such different stability concepts at the continuum level for freestanding graphene. Our approach here is that of possibly considering *all* small perturbations, where such smallness is exclusively aimed at preserving the local coordination of the atomic bonds. As a consequence, the stability criterion here addressed turns out to be the most restrictive. The reader is referred to [18, 40] for related stability analysis for other carbon nanostructures, including carbyne, graphene, the fullerene C_{60}, and diamond. Moving from the present analysis, a refined analytic discussion of the stability of carbon nanotobes under moderate stretching has been developed in [17].

Under some classical choice of interaction potentials, we investigate first the minimization of the configurational energy in specific one-parameter classes of periodic zigzag and armchair configurations which include the classical *rolled-up* [10] and the *polyhedral* [6] model. Here, the dimensionality of the problem scales down and we can prove that a unique optimal configuration exists. Quite remarkably, this optimal configuration does not coincide neither with the classical rolled-up [10] nor with the polyhedral model [6]. Our analysis thus entails that these classical geometrical models do not admit a variational interpretation and that energy minimality induces a different structure.

The stability of such optimal configurations with respect to general small perturbations has been already computationally ascertained in [30]. Our aim here is to provide some analytical justification of this fact. In particular, we prove stability with respect to a large class of small perturbations including tractions and diameter dilations, among many others. Moreover, we propose an *ansatz*, namely, (5), under which stability can be proved for *all* small perturbations. Numerical evidence for the validity of such assumption is provided.

This path is of course not new to computational chemists, and numerical investigations of carbon-nanotube geometries at the single-atom level are already available [37, 38, 39, 47]. With respect to the current stand the novelty of our contribution is twofold. On the one hand, we investigate the full structure at once, by dropping the periodicity assumption on perturbations. On the other hand, we obtain rigorous analytical results instead of numerical assessments. Note that a menagerie of different possible choices for energy terms has been implemented in computational chemistry codes [3, 5, 19, 31, 45]. By sorting out a set of minimal hypothesis of the configurational energy we are hence contributing to cross-validate these choices in view of their capability of describing stable carbon-nanotube geometries.

The plan of the paper is the following. We devote section 2 to the specification of the mathematical setting and the statement of the main stability result. The specific geometry of periodic zigzag and armchair configurations is then detailed in section 3. We analyze energy minimization at single atoms in section 4 and identify optimal configurations, whose stability is then proved in section 5 by means of convexity and monotonicity arguments. Eventually, we devote section 6 to a numerical assessment of ansatz (5).

2. Main result. In this section we introduce the mathematical setting and state the main result of the paper, namely, Theorem 2.1. *Nanotubes* are described as collections of distinct points in $\mathbb{R}^3$ of the form

$$\mathcal{C} := C_n + L\mathbb{Z}\, e_3.$$

The set $C_n := \{x_1, \dots, x_n\}$ is called the *n-cell* of the nanotube $\mathcal{C}$, where the points $x_i \in \mathbb{R}^3$ are such that $x_i \cdot e_3 \in [0, L)$. The possibly very large $L > 0$ acts as *period* of the nanotube along its *axis* $e_3 := (0, 0, 1)$ and is here introduced for the sake of definiteness only. In particular, such periodicity is immaterial with respect to the fine, local geometry of the nanotube which is here analyzed, and it is introduced just to prevent the need of discussing the boundary effects due to finite capping. Note that nanotubes can be as long as 10^6 times their diameter, so that L would ideally correspond to such length. In the following, we systematically identify the nanotube $\mathcal{C}$ with the pair (C_n, L).

To each nanotube $\mathcal{C}$ we associate a *configurational energy* $E(\mathcal{C})$. This is modeled on the specific phenomenology of sp^2 covalent bonding of carbon atoms [4]. In particular, bonds of a specific length (here normalized to 1) and bond angles of $2\pi/3$ and $4\pi/3$ are favored. Correspondingly, the energy E features the sum of a two- and a three-body contribution and reads

$$E(\mathcal{C}) = E(C_n, L) := \frac{1}{2} \sum_{(i,j)\in\mathcal{N}} v_2(|x_i - x_j|_L) + \frac{1}{2} \sum_{(i,j,k)\in\mathcal{T}} v_3(\omega_{ijk}), \tag{1}$$

the two terms being described in the following.

The *two-body potential* $v_2 : \mathbb{R}^+ \to [-1, \infty)$ is assumed to be minimized only in 1 and its minimal value is fixed to be $v_2(1) = -1$, with no loss of generality. Moreover, v_2 is asked to be *short-ranged*, i.e., to be supported in a neighborhood of 1 of the form $(0, \rho)$. For the sake of definiteness, we let $v_2(r) = 0$ for $r > \rho$ with $\rho := 1.1$. By introducing the *distance modulo L* defined by

$$|x_i - x_j|_L := \min_{z\in\{-1,0,+1\}} |x_i - x_j + Lze_3|,$$

we say that two points $x_i, x_j \in C_n$, $i \neq j$, are *bonded*, or that the bond between x_i and x_j is *active*, if $|x_i - x_j|_L < \rho$, and we refer to the graph formed by all the active bonds as the *bond graph*. Let us denote by $\mathcal{N}$ the set of all pairs of indexes corresponding to bonded points, i.e.,

$$\mathcal{N} := \{(i, j) \,:\, x_i, x_j \in C_n,\, i \neq j, \text{ and } |x_i - x_j|_L < \rho\}.$$

For $x_j \in C_n$ we also let

$$\mathcal{N}(x_j) := \{i \in \{1, \dots, n\} : (i, j) \in \mathcal{N}\},$$

and if $i \in \mathcal{N}(x_j)$, we define by x_i^j the point in $\{x_i + Lze_3 \,:\, z = -1, 0, +1\}$ such that $|x_i^j - x_j| = |x_i - x_j|_L$.

The *three-body potential* $v_3 : [0, 2\pi] \to [0, \infty)$ is assumed to be symmetric around π, namely, $v_3(\alpha) = v_3(2\pi - \alpha)$, and to attain minimum value 0 only at $2\pi/3$ and $4\pi/3$. Furthermore, v_3 is required to be convex and strictly decreasing in the interval

$$I_\varepsilon := (2\pi/3 - \varepsilon, 2\pi/3] \tag{2}$$

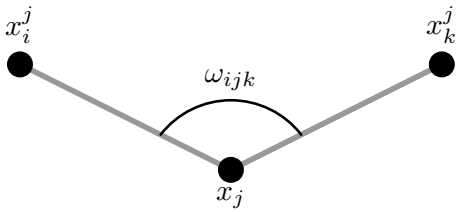

FIG. 2. *Notation for bonds and bond angles.*

for some given $\varepsilon < \pi/8$, and twice differentiable at each point of I_ε, with continuous second derivative. This entails that $v_3'(2\pi/3) = 0$. Moreover, we additionally assume that $v_3''(2\pi/3) > 0$. The parameter ε will be assumed to be fixed throughout the paper. The index set $\mathcal{T}$ in (1) identifies triples of first-neighboring points, namely,

$$\mathcal{T} := \{(i,j,k) \,:\, x_i, x_j, x_k \in C_n,\, i \neq k,\, i \in \mathcal{N}(x_j) \text{ and } k \in \mathcal{N}(x_j)\}.$$

For $(i,j,k) \in \mathcal{T}$, the *bond angle* ω_{ijk} in (1) is the angle formed by the vectors $x_i^j - x_j$ and $x_k^j - x_j$ (counterclockwise oriented with respect to the normal $(x_i^j - x_j) \wedge (x_k^j - x_j)$); see Figure 2.

The above assumptions on v_2 and v_3 are quite general. In particular, they are satisfied by standard interaction potentials for sp^2-bonding in carbon [41, 42]. Note that we do not require v_2 to be repulsive at short-range, although this is a fairly classical assumption and, currently, the only frame in which crystallization in the hexagonal lattice has been rigorously proved [11, 16, 29]. Since the energy E is clearly rotation and translation invariant, in the following we will tacitly assume that all statements are to be considered up to isometries.

We aim at characterizing the fine geometry of *stable* nanotubes, namely, those which locally minimize the configurational energy E. To this end, we need to introduce specific families of zigzag and armchair nanotubes, denoted by $\mathscr{F}_\ell^z$ and $\mathscr{F}_\ell^a$ in the following, where $\ell \in \mathbb{N}$ stands for the roll-up parameter whose role we discussed in the introduction; see Figure 1. For the sake of convenience we postpone to section 3 the detailed definition of such families. Let us however anticipate that all nanotubes in $\mathscr{F}_\ell^s$ (throughout the paper we use the index $s = z$ for zigzag and $s = a$ for armchair) are *objective* configurations [23], for they can be obtained as orbits of two points under the action of an isometry group of rotations and translations. In particular, nanotubes in $\mathscr{F}_\ell^s$ all have points disposed on sections orthogonal to their axis, each containing exactly $\ell \in \mathbb{N}$ points, and the topology of their bond graph corresponds to that of the hexagonal lattice $\mathcal{H}$ under the identification $x \mapsto x + \ell a$ for zigzag and $x \mapsto x + \ell(a+b)$ for armchair, as seen in the introduction.

For a given $\ell \in \mathbb{N}$, the collection $\mathscr{F}_\ell^s$ can be described by a single scalar parameter. As a consequence, when restricted to the specific family $\mathscr{F}_\ell^s$ of nanotubes, the minimization of the configurational energy is reduced to a scalar problem. Under the above assumptions one can prove that a unique strict minimizer $\mathcal{F}_\ell^s$ exists in $\mathscr{F}_\ell^s$. We prove this in Theorem 4.4 by slightly extending the former [30, Thms. 4.3 and 6.1]. Let us mention again that these minimizers do not coincide with the classical rolled-up [10] nor with the polyhedral model [6]; see [30, Thms. 4.1-2 and 6.1], which however belong to these families.

The focus of this paper is to prove that the objective nanotubes $\mathcal{F}_\ell^s$ are stable, namely, that they locally minimize the energy with respect to *general* perturbations,

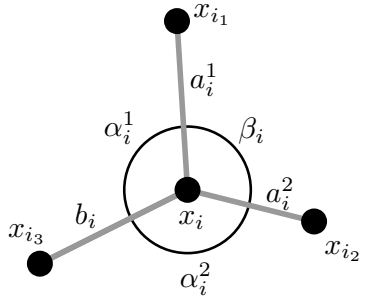

FIG. 3. *Angles and bonds at the point $x_i \in C_n$.*

not restricting to $\mathscr{F}_\ell^s$. In order to illustrate the statement, let $\ell \in \mathbb{N}$ be fixed and denote by $F_n^s = \{x_1^s, \dots, x_n^s\}$ and L^s the n-cell and the period of $\mathcal{F}_\ell^s$, so that $\mathcal{F}_\ell^s = (F_n^s, L^s)$. We define *small perturbations* $\mathscr{P}_\eta(\mathcal{F}_\ell^s)$ of $\mathcal{F}_\ell^s$ as

$$\mathscr{P}_\eta(\mathcal{F}_\ell^s) := \{\widetilde{\mathcal{F}} = (F_n, L) \ : \ F_n := \{x_1, \dots, x_n\} \quad \text{and} \quad L := L^s + \delta L \\ \text{with } x_i := x_i^s + \delta x_i \text{ for } |\delta x_i| < \eta \text{ and } |\delta L| < \eta\}.$$

The parameter $\eta > 0$ will be always chosen to be small enough so that the topology of the bond graph of a nanotube $\widetilde{\mathcal{F}} \in \mathscr{P}_\eta(\mathcal{F}_\ell^s)$ coincides with that of $\mathcal{F}_\ell^s$: in particular, if η is small enough, we have

$$\mathcal{N}(x_i) = \mathcal{N}(x_i^s), \qquad i = 1, \dots, n. \tag{3}$$

For all nanotubes whose n-cell $C_n = \{x_1, \dots, x_n\}$ fulfills (3), in particular for all perturbations $\widetilde{\mathcal{F}} \in \mathscr{P}_\eta(\mathcal{F}_\ell^s)$ with small enough η, we have $\#\mathcal{N}(x_i) = 3$ and we denote by i_1, i_2, i_3 the three elements of $\mathcal{N}(x_i)$ for any $i \in \{1, \dots, n\}$. Moreover, we indicate by $b_i = |x_i - x_{i_3}|$ and $a_i^j = |x_i - x_{i_j}|$, $j = 1, 2$, the lengths of the three bonds at x_i. The bond angle (smaller than or equal to π) between a_i^1 and a_i^2 will be denoted by β_i whereas α_i^j are the bond angles (smaller than or equal to π) between b_i and a_i^j for $j = 1, 2$; see Figure 3. This notation will be used to highlight the role of the bond b_i: this will (approximately) be parallel to the axis for zigzag nanotubes and (approximately) lay on a plane perpendicular to the axis for armchair nanotubes.

Given $x_i \in C_n$ with $\mathcal{N}(x_i) = \{i_1, i_2, i_3\}$, the full three-dimensional geometry of its first neighbors can be uniquely determined up to rotations in terms of the bond lengths (a_i^1, a_i^2, b_i) and the bond angles $(\alpha_i^1, \alpha_i^2, \beta_i)$. In fact, the angle β_i can be expressed as a function of α_i^1, α_i^2, and an additional angle γ_i^s, whose definition differs in the zigzag and in the armchair case. Indeed, we let γ_i^z be the (smaller than π) angle formed by the plane containing x_i, x_{i_1}, and x_{i_3} and the plane containing x_i, x_{i_2}, and x_{i_3}, and γ_i^a is the (larger than $\pi/2$) angle between the line $x_i - x_{i_3}$ and its projection on the plane containing x_i, x_{i_1}, and x_{i_2} (see Figure 4).

We indicate by γ_ℓ the internal angle of the regular (2ℓ)-gon, namely,

$$\gamma_\ell := \pi(1 - 1/\ell).$$

Given a nanotube $\widetilde{\mathcal{F}} \in \mathscr{P}_\eta(\mathcal{F}_\ell^s)$ with small enough η so that (3) holds, let $\overline{\gamma}$ be the mean of its γ_i^s angles, namely,

$$\overline{\gamma} := \frac{1}{n} \sum_{i=1}^{n} \gamma_i^s \tag{4}$$

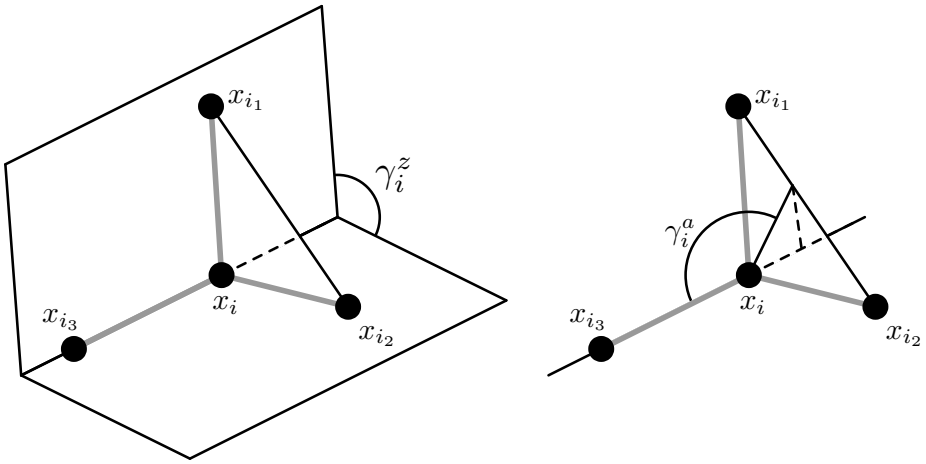

FIG. 4. *Angles γ_i^z and γ_i^a at the point $x_i \in C_n$ are illustrated on the left and on the right, respectively. Note that the two dashed lines in the right picture are perpendicular.*

with s either a or z. We note that $\overline{\gamma} = \gamma_\ell$ if $\widetilde{\mathcal{F}} \in \mathscr{F}_\ell^s$. Indeed, nanotubes in $\mathscr{F}_\ell^s$ are contained in the surface of a prism (see section 3 below), whose section is a (2ℓ)-gon, and the sum of the γ_i^s is related with the sum of the internal angles of such (2ℓ)-gon. On the other hand, $\overline{\gamma} \neq \gamma_\ell$ in general.

We are now ready to state our main result.

THEOREM 2.1 (stability). *Let $\varepsilon \in (0, \pi/8)$. There exists $\ell_\varepsilon^s = \ell_\varepsilon^s(v_3, \varepsilon) \in \mathbb{N}$ such that for all $\ell > \ell_\varepsilon^s$ one can find $\eta_\varepsilon^s = \eta_\varepsilon^s(v_3, \varepsilon, \ell) > 0$ so that any nontrivial perturbation $\widetilde{\mathcal{F}} \in \mathscr{P}_{\eta_\varepsilon^s}(\mathcal{F}_\ell^s)$ with $\overline{\gamma} \leq \gamma_\ell$ satisfies $E(\widetilde{\mathcal{F}}) > E(\mathcal{F}_\ell^s)$.*

The theorem asserts the local minimality of $\mathcal{F}_\ell^s$ with respect to all small perturbations with $\overline{\gamma} \leq \gamma_\ell$. As already mentioned, this class includes all small perturbations in $\mathscr{F}_\ell^s$, which indeed fulfill the stronger $\overline{\gamma} = \gamma_\ell$. This particularly implies that Theorem 2.1 includes the former analysis in [30], which is restricted to perturbations in $\mathscr{F}_\ell^s$.

More significantly, a large class of small perturbations which are *not* in $\mathscr{F}_\ell^s$ fulfill the constraint $\overline{\gamma} \leq \gamma_\ell$ as well. In the zigzag case, one even has $\overline{\gamma} = \gamma_\ell$ whenever the perturbation preserves the alignment to the nanotube axis of the b_i bonds. This includes tractions and diameter changes, which may vary section by section of the nanotube. Moreover, sections can be deformed, for instance, squeezed to ellipses, and some shear can also be accommodated, all possibly varying section by section. The armchair case is analogous: a large class of relevant perturbations including traction and diameter change fulfill $\overline{\gamma} \leq \gamma_\ell$.

Unfortunately not all small perturbations have $\overline{\gamma} \leq \gamma_\ell$. One example is obtained by displacing a single point of $\mathcal{F}_\ell^s$ orthogonally to the axis. The assertion of Theorem 2.1 can be extended to *all* small perturbations under the following assumption: given ℓ, η_ε^s from Theorem 2.1,

$$\forall \widetilde{\mathcal{F}} \in \mathscr{P}_{\eta_\varepsilon^s}(\mathcal{F}_\ell^s),\ \exists\, \overline{\mathcal{F}} \in \mathscr{P}_{\eta_\varepsilon^s}(\mathcal{F}_\ell^s) \text{ such that } \overline{\gamma} \leq \gamma_\ell \text{ and } E(\widetilde{\mathcal{F}}) \geq E(\overline{\mathcal{F}}), \tag{5}$$

where $\overline{\gamma}$ is the mean value of the γ_i^s angles of $\overline{\mathcal{F}}$. The latter has a constructive flavor:

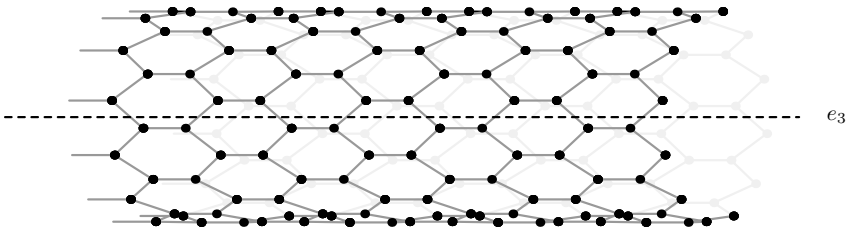

FIG. 5. *A zigzag nanotube in* $\mathscr{F}^z_{12}$.

for all given small perturbations one is required to exhibit a better energy competitor fulfilling the constraint $\overline{\gamma} \leq \gamma_\ell$. We advance two such candidate energy-reducing constructions and present numerical evidence for (5) in section 6.

The statement of Theorem 2.1 relates the size of ℓ, which roughly corresponds to the diameter of the nanotube, and the parameter ε, which instead measures the interval of validity of the assumptions on v_3. The smaller the ε, namely, the weaker the hypothesis on v_3, the larger the diameter of the nanotube needs to be in order have stability. At the same time, nanotubes of very small diameter may be treated if assumptions on v_3 are strengthened, namely, if ε is large enough.

3. Zigzag and armchair geometries. We devote this section to the description of the geometry of zigzag and armchair nanotubes and, specifically, we define the families $\mathscr{F}^s_\ell$.

Zigzag. For any $\ell > 3$, the family $\mathscr{F}^z_\ell$ is defined up to isometries as

(6)
$$\left\{ \left(r\cos\left(\frac{\pi(2i+k)}{\ell}\right), r\sin\left(\frac{\pi(2i+k)}{\ell}\right), k(1+s)+j \right) \;\middle|\; i=1,\dots,\ell,\ j=0,1,\ k\in\mathbb{Z} \right\}$$

for some choice of radius r and step $1+s$ so that

$$r \in \left(0,\ \frac{1}{2\sin(\pi/(2\ell))}\right) \quad \text{and} \quad s \in (0,1)$$

along with the constraint

$$s^2 + 4r^2 \sin^2\left(\frac{\pi}{2\ell}\right) = 1. \tag{7}$$

Figure 5 illustrates a configuration in $\mathscr{F}^z_\ell$. As already mentioned, configurations in $\mathscr{F}^z_\ell$ are objective [23] for they correspond to orbits of two points under translations along e_3 of $2(1+s)$ and rototranslations in direction e_3 of angle π/ℓ and length $1+s$. The constraint (7) expresses the fact that all bonds have length 1, and we have that $\mathscr{F}^z_\ell$ is a one-parameter smooth family of configurations: each configuration in $\mathscr{F}^z_\ell$ is uniquely determined by specifying either r or s. Note that for $r=0$ the cylinder is reduced to its axis and for $s=0$ the sections collide.

Nanotubes $\mathcal{F}$ in $\mathscr{F}^z_\ell$ have all points lying on the surface of a cylinder with axis e_3 and radius r and are organized in planar sections, perpendicular to e_3, obtained by fixing k and j in (6). Each section contains exactly ℓ points are arranged at the vertices of a regular ℓ-gon, and its two closest sections are at distance s and 1, respectively.

The position of any point in $\mathcal{F}$ is identified by the triple (i,k,j) for $i \in \{1,\dots,\ell\}$, $k \in \mathbb{Z}$, and $j \in \{0,1\}$. The point (i,k,j) is bonded to the three points $(i,k,1)$, $(i,k-1,1)$, and $(i-1,k-1,1)$ for $j=0$, or the three points $(i,k,0)$, from $(i,k+1,0)$ and $(i-1,k+1,0)$ for $j=1$ (along with the convention that $(0,k,j)$ and (ℓ,k,j) are identified), since they are at distance 1. The full geometry of such three neighbors to x_i is hence described by the three angles $(\alpha_i^1,\alpha_i^2,\beta_i)$; see Figure 3. Equivalently, one can express β_i as a function of α_i^1, α_i^2 and γ_i^z as

$$\beta_i = \tilde\beta^z\left(\alpha_i^1,\alpha_i^2,\gamma_i^z\right),$$

where the function $\tilde\beta^z$ is defined by

$$\tilde\beta^z(\alpha^1,\alpha^2,\gamma) := 2\arcsin\left(\sqrt{(1-\sin\alpha^1\sin\alpha^2\cos\gamma-\cos\alpha^1\cos\alpha^2)/2}\right). \tag{8}$$

In case $\alpha^1=\alpha^2$ we will also use the notation

$$\beta^z(\alpha,\gamma) := \tilde\beta^z(\alpha,\alpha,\gamma) = 2\arcsin\left(\sin\alpha\sin\frac{\gamma}{2}\right).$$

Restrictions on the possible choice of the radius r have to be introduced in order to ensure that bond graph of nanotubes in $\mathscr{F}_\ell^z$ to locally have the topology of Figure 4. This imposes to rule out extremal values of the radius r. At first, sections of the nanotube should be wide enough to have that second-neighbors stay at distance larger than $\rho = 1.1$. This translates to

$$r > r_-^z := \frac{0.55}{\sin\gamma_\ell}. \tag{9}$$

On the other hand, if r is large, then the intersectional distance $1+s$ approaches 1, thus activating extra bonds. This calls for the condition

$$r < r_+^z := \frac{\sqrt{0.9975}}{2\sin(\pi/(2\ell))} \tag{10}$$

as already discussed in [30]. We record all relevant facts about the family $\mathscr{F}_\ell^z$ in the following statement.

PROPOSITION 3.1 (zigzag geometry). *In $\mathcal{F} \in \mathscr{F}_\ell^z$ with radius $r \in (r_-^z, r_+^z)$ all points have exactly three (first-nearest) neighbors, all at distance 1, with one bond b aligned with e_3. The two bond angles (smaller than π) formed by b are equal and have value $\alpha \in (\pi/2,\pi)$. The third bond angle (smaller than π) is*

$$\beta^z(\alpha,\gamma_\ell) = 2\arcsin\left(\sin\alpha\sin\frac{\gamma_\ell}{2}\right).$$

We refer to [30, Prop. 3.2] for a detailed proof of Proposition 3.1. Let us point out here that, by (7) and the fact that $\sin\alpha = \sqrt{1-s^2} = 2r\sin(\pi/(2\ell))$, the family $\mathscr{F}_\ell^z$ is smoothly and uniquely determined not only by the parameters r and s independently,

but also by the angle α. In this regard note that the constraints on α corresponding to (10) is

$$\alpha > \alpha^z_- := \arccos(-1/20) \approx 93^\circ, \tag{11}$$

and the one corresponding to (9) is

$$2\sin\alpha\sin(\gamma_\ell/2) > \rho.$$

For all $\ell \geq 4$ the latter is implied by the following:

$$\alpha < \alpha^z_+ := \pi - \arcsin\left(1.1/\sqrt{2+\sqrt{2}}\right) \approx 143.5^\circ. \tag{12}$$

Proposition 3.1 entails in particular that, for all $\alpha \in (\alpha^z_-, \alpha^z_+)$, a configuration $\mathcal{F}_\alpha \in \mathscr{F}^z_\ell$, uniquely defined by its bond angle α, features two thirds of the bond angles (smaller than π) with value α and one third with value $\beta^z(\alpha, \gamma_\ell)$. This allows a simple expression for its energy. Denote its n-cell ($n = 4m\ell$ for some $m \in \mathbb{N}$) by F_n and observe that its period L can can be computed as

$$L = 2m(1 - \cos\alpha). \tag{13}$$

(For $m = 1$ we get the minimal period of the configuration.) As all points bring the same contribution to the energy we have

$$E(\mathcal{F}_\alpha) = E(F_n, L) = -\frac{3}{2}n + n\mathcal{E}^z(\alpha, \gamma_\ell), \tag{14}$$

where

$$\mathcal{E}^z(\alpha, \gamma) := 2v_3(\alpha) + v_3(\beta^z(\alpha, \gamma)).$$

Armchair. For all $\ell \in 2\mathbb{N}$, we introduce the family $\mathscr{F}^a_\ell$ up to isometries as

$$\left\{ \left(r\cos\left(\frac{2\pi}{\ell}(2i+k)+q_r j\right), r\sin\left(\frac{2\pi}{\ell}(2i+k)+q_r j\right), pk\right) \,\middle|\, i = 1, \dots, \frac{\ell}{2},\ j = 0, 1,\ k \in \mathbb{Z} \right\} \tag{15}$$

for some choice of radius r and step p such that

$$r \in \left(\frac{1}{2\sin(\pi/\ell)}, \frac{1}{2\sin(\pi/(2\ell))}\right) \quad \text{and} \quad p \in (0, 1),$$

and the following constraint holds:

$$p^2 + 4r^2\sin^2\left(\frac{\pi}{\ell} - \frac{q_r}{2}\right) = 1, \tag{16}$$

where

$$q_r := 2\arcsin\left(\frac{1}{2r}\right).$$

Points in $\mathcal{F} \in \mathscr{F}^a_\ell$ lie on the surface of a cylinder with radius r and axis e_3, and they are arranged in planar sections, perpendicular to e_3, obtained by fixing k and j in (15). The constraint (16) entails that all bonds have length 1. The collection $\mathscr{F}^a_\ell$ is

a one-parameter smooth family uniquely determined by r or p. The limit cases $p = 0$ (for which we have $q_r = \pi/\ell$) and $p = 1$ (for which $q_r = 2\pi/\ell$) correspond to having the sections on the same plane, and to a prism shape, respectively.

Each of the sections exactly contains ℓ points, arranged at the vertices of two regular $(\ell/2)$-gons, which are rotated of an angle q_r with respect to each other. For each section, the two closest sections are both at distance p. Nanotubes $\mathscr{F}^a_\ell$ are objective [23], for they correspond to the orbit of two points under rotations of $4\pi/\ell$ around the axis e_3 and rototranslations about e_3 of angle $2\pi/\ell$ and step p. By (15) we see that the triple (i,k,j) for $i \in \{1,\dots,\ell/2\}$, $k \in \mathbb{Z}$, and $j \in \{0,1\}$ uniquely determines the positions of all points. Note that the point (i,k,j) is bonded with the three points $(i,k,1)$, $(i,k-1,1)$, and $(i-1,k+1,1)$ for $j = 0$, or the three points $(i,k,0)$, $(i,k+1,0)$, and $(i+1,k-1,0)$ for $j = 1$ (where we identify $(0,k,j)$ and $(\ell/2,k,j)$), since they are at distance 1. The geometry of such an ensemble of three neighbors to x_i is hence described by the three angles $(\alpha^1_i, \alpha^2_i, \beta_i)$; see Figure 4. Equivalently, one can express β_i as a function of α^1_i, α^2_i, and γ^a_i as

$$\beta_i = \tilde{\beta}^a\left(\alpha^1_i, \alpha^2_i, \gamma^a_i\right),$$

where the function $\tilde{\beta}^a$ is defined by

$$\tilde{\beta}^a\left(\alpha^1, \alpha^2, \gamma\right) := \arccos\left(\frac{\cos\alpha^1}{\cos\gamma}\right) + \arccos\left(\frac{\cos\alpha^2}{\cos\gamma}\right).$$

If $\alpha^1 = \alpha^2$ we will also use the notation

$$\beta^a(\alpha,\gamma) := \tilde{\beta}^a\beta_2(\alpha,\alpha,\gamma) = 2\arccos\left(\frac{\cos\alpha}{\cos\gamma}\right).$$

As in the case of zigzag geometries, parameters should be additionally constrained in order the bond graph to locally have the topology of Figure 4. Since p is the distance between two consecutive sections we require $2p > \rho$. According to (16) this corresponds to $2r\sin(\pi/\ell - q_r/2) < \sqrt{0.6975}$, which yields $r < r^a_+$, where r^a_+ denotes the unique positive solution of the corresponding equality. (Notice that the map $r \mapsto 2r\sin(\pi/\ell - q_r/2)$ is monotone increasing for $r > 1/2$, as $\ell \geq 4$, and takes values 0 and 1 at extremes of the definition range for r.)

On the other hand, the distance between two nearest points on a section is either $2r\sin(q_r/2) = 1$ or $2r\sin(2\pi/\ell - q_r/2)$. We impose the latter to be greater than ρ to avoid an extra bond. This requires $r > r^a_-$, where r^a_- is the unique positive solution to $2r\sin(2\pi/\ell - q_r/2) = \rho$. The armchair version of Proposition 3.1 reads as follows.

PROPOSITION 3.2 (armchair geometry). *In $\mathcal{F} \in \mathscr{F}^a_\ell$ with radius $r \in (r^a_-, r^a_+)$ all points have exactly three (first-nearest) neighbors, all at distance* 1*, with one bond b orthogonal to e_3. The two bond angles (smaller than π) formed by b are equal and have value $\alpha \in (\pi/2, \pi)$. The third bond angle (smaller than π) is*

$$\beta^a(\alpha,\gamma_\ell) = 2\arccos\left(\frac{\cos\alpha}{\cos\gamma_\ell}\right).$$

Analogously as for the zigzag family, by the equation

$$\cos\alpha = 2r\cos\gamma_\ell\sin\left(\frac{\pi}{\ell} - \frac{q_r}{2}\right)$$

one can characterize the element of the family $\mathscr{F}_\ell^a$ via the bond angle $\alpha \in (\pi/2, \gamma_\ell)$. The constraint $r < r_+^a$ is equivalent to

$$\cos^2 \alpha < 0.6975 \cos^2 \gamma_\ell, \tag{17}$$

which, for all $\ell \geq 4$, is implied by

$$\alpha < \alpha_+^a := \arccos(-\sqrt{0.34875}) \approx 126^\circ. \tag{18}$$

On the other hand, using the identity $2r \sin(2\pi/\ell - q_r/2) = 1 + 4r \cos(\pi/\ell) \sin(\pi/\ell - q_r/2)$ and (17), the constraint $r > r_-^a$ translates to

$$\alpha > \alpha_-^a := \arccos(-1/20) \approx 93^\circ. \tag{19}$$

For all $\alpha \in (\alpha_-^a, \alpha_+^a)$ the energy of the nanotube $\mathcal{F}_\alpha \in \mathscr{F}_\ell^a$ has a simple expression, since all points contribute the same amount to it. For $\mathcal{F}_\alpha = (F_n, L)$, where $n = 2m\ell$, $m \in \mathbb{N}$, we can compute that

$$L := 2m \left(1 - \frac{\cos^2 \alpha}{\cos^2 \gamma_\ell}\right)^{1/2} \tag{20}$$

and the energy reads

$$E(\mathcal{F}_\alpha) = E(F_n, L) = -\frac{3}{2} n + n \mathcal{E}^a(\alpha, \gamma_\ell), \tag{21}$$

where

$$\mathcal{E}^a(\alpha, \gamma) := 2v_3(\alpha) + v_3(\beta^a(\alpha, \gamma)).$$

4. Angle-energy optimization. The analysis of the previous section entails that the minimization problem for configurations in $\mathscr{F}_\ell^s$ is localized, for all points equally contribute to the energy. As all bond lengths in $\mathscr{F}_\ell^s$ are equal to 1, we reduce ourselves to the study of a scalar functional corresponding to the angle energy of a single point; see (14) and (21). This analysis is performed in this section and, in particular, brings to the identification of the optimal configuration $\mathcal{F}_\ell^s$.

Let us start by computing the derivatives of the functions $\tilde{\beta}^s$, which we consider to be defined in $(\pi/2, 3\pi/4) \times (\pi/2, 3\pi/4) \times [3\pi/4, \pi]$. These values are just taken for the sake of definiteness and could be differently chosen around $2\pi/3$ for α^1, α^2 and left to π for γ. Notice in particular that $\gamma_\ell \in [3\pi/4, \pi)$ for $\ell \geq 4$. In this range, we have

$$\begin{aligned}
\partial_{\alpha^1} \tilde{\beta}^z \left(\alpha^1, \alpha^2, \gamma\right) &= \frac{-\cos\alpha^1 \sin\alpha^2 \cos\gamma + \sin\alpha^1 \cos\alpha^2}{\sqrt{1 - (\sin\alpha^1 \sin\alpha^2 \cos\gamma + \cos\alpha^1 \cos\alpha^2)^2}} < 0, \\
\partial_{\alpha^2} \tilde{\beta}^z \left(\alpha^1, \alpha^2, \gamma\right) &= \frac{-\sin\alpha^1 \cos\alpha^2 \cos\gamma + \cos\alpha^1 \sin\alpha^2}{\sqrt{1 - (\sin\alpha^1 \sin\alpha^2 \cos\gamma + \cos\alpha^1 \cos\alpha^2)^2}} < 0, \\
\partial_{\alpha^i} \tilde{\beta}^a \left(\alpha^1, \alpha^2, \gamma\right) &= -\frac{2\sin\alpha^i}{\sqrt{\cos^2\gamma - \cos^2\alpha^i}} < 0, i = 1, 2.
\end{aligned} \tag{22}$$

The functions $\beta^s(\alpha,\gamma)$ are smooth on $(\pi/2,3\pi/4)\times[3\pi/4,\pi]$, and we have

$$\partial_\alpha\beta^z = \frac{2\sin(\gamma/2)\cos\alpha}{\sqrt{1-\sin^2\alpha\sin^2(\gamma/2)}} < 0, \quad \partial^2_{\alpha\alpha}\beta^z = -\frac{2\sin\alpha\sin(\gamma/2)\cos^2(\gamma/2)}{(1-\sin^2\alpha\sin^2(\gamma/2))^{3/2}} < 0,$$

(23)

$$\partial_\gamma\beta^z = \frac{\sin\alpha\cos(\gamma/2)}{\sqrt{1-\sin^2\alpha\sin^2(\gamma/2)}} > 0, \quad \partial^2_{\gamma\gamma}\beta^z = -\frac{\sin\alpha\cos^2\alpha\sin(\gamma/2)}{2(1-\sin^2\alpha\sin^2(\gamma/2))^{3/2}} < 0,$$

$$\partial_\alpha\beta^a = -\frac{2\sin\alpha}{\sqrt{\cos^2\gamma-\cos^2\alpha}} < 0, \quad \partial^2_{\alpha\alpha}\beta^a = \frac{2\cos\alpha\sin^2\gamma}{(\cos^2\gamma-\cos^2\alpha)^{3/2}} < 0,$$

(24)

$$\partial_\gamma\beta^a = \frac{2\cos\alpha\tan\gamma}{\sqrt{\cos^2\gamma-\cos^2\alpha}} > 0, \quad \partial^2_{\gamma\gamma}\beta^a = \frac{2\cos\alpha(\cos^2\gamma-\cos^2\alpha+\sin^2\gamma\cos^2\gamma)}{\cos^2\gamma(\cos^2\gamma-\cos^2\alpha)^{3/2}} < 0.$$

The values at the extrema of the definition range are

$$\partial_\alpha\beta^z(2\pi/3,\pi) = -2, \quad \partial^2_{\alpha\alpha}\beta^z(2\pi/3,\pi) = 0,$$

(25)
$$\partial_\gamma\beta^z(2\pi/3,\pi) = 0, \quad \partial^2_{\gamma\gamma}\beta^z(2\pi/3,\pi) = -\sqrt{3}/2,$$

$$\partial_\alpha\beta^a(2\pi/3,\pi) = -2, \quad \partial^2_{\alpha\alpha}\beta^a(2\pi/3,\pi) = 0,$$

(26)
$$\partial_\gamma\beta^a(2\pi/3,\pi) = 0, \quad \partial^2_{\gamma\gamma}\beta^a(2\pi/3,\pi) = -2/\sqrt{3}.$$

Let us consider first the case in which two of the three bond angles are equal. In particular, we discuss the minimization of $\mathcal{E}^s$ with respect to α for all given γ. Some care is needed for the choice of the interval of optimization. This has to be specified depending on γ and $\varepsilon\in(0,\pi/8)$ from (2) in order to ensure that v_3 is evaluated just in I_ε, namely, where the assumptions hold. For $\varepsilon\in(0,\pi/8)$ and $\gamma\in[3\pi/4,\pi]$ we define the two quantities

(27)
$$\sigma^z_\varepsilon(\gamma) := \pi - \arcsin\left(\frac{\sin(\pi/3-\varepsilon/2)}{\sin(\gamma/2)}\right), \qquad \sigma^a_\varepsilon(\gamma) := \arccos(\cos\gamma\cos(\pi/3-\varepsilon/2)).$$

From the definitions of β^s and their monotonicity properties from (23), (24), it is not difficult to check that $\sigma^s_\varepsilon(\gamma)$ belongs to $(\pi/2,3\pi/4)$ and that it is the unique solution to the equation $\beta^s(\cdot,\gamma) = 2\pi/3-\varepsilon$ on $(\pi/2,3\pi/4)$. Moreover, we have $\beta^s(\alpha,\gamma) > 2\pi/3-\varepsilon$ if $\alpha<\sigma^s_\varepsilon(\gamma)$. The functions $\sigma^s_\varepsilon(\gamma)$ are strictly increasing both with respect to $\varepsilon\in(0,\pi/8)$ and to $\gamma\in[3\pi/4,\pi]$.

By recalling that ε is fixed throughout, one has that $\sigma^s_\varepsilon(\gamma)$ is larger than $2\pi/3$ if γ is large enough (i.e., close to π). More precisely, taking into account the strict monotonicity of $[3\pi/4,\pi]\ni\gamma\mapsto\sigma^s_\varepsilon(\gamma)$, we define values γ^s_ε as follows:

$$\gamma^s_\varepsilon := \begin{cases} 3\pi/4 & \text{if } \sigma^s_\varepsilon(3\pi/4)\geq 2\pi/3, \\ (\sigma^s_\varepsilon)^{-1}(2\pi/3) & \text{if } \sigma^s_\varepsilon(3\pi/4)<2\pi/3, \end{cases}$$

where $(\sigma^s_\varepsilon)^{-1}(\cdot)$ is the inverse of $\sigma^s_\varepsilon(\cdot)$ on $[3\pi/4,\pi]$. In this way, we obtain $\sigma^s_\varepsilon(\gamma)>2\pi/3$

if $\gamma \in (\gamma_\varepsilon^s, \pi)$. It will hence be important to keep γ in the range $(\gamma_\varepsilon^s, \pi)$. Notice that the smaller the ε, the stronger is the restriction on the values of γ. For instance, if $\varepsilon = \pi/12$, we have $\gamma_\varepsilon^z = 3\pi/4$ and $\gamma_\varepsilon^a \in (3\pi/4, 5\pi/6)$.

We will also need the quantities $\sigma_0^s(\gamma)$, defined as the unique solutions to $\beta^s(\cdot,\gamma) = 2\pi/3$ on $(\pi/2, 3\pi/4)$. These are explicitly given by

$$\sigma_0^z(\gamma) := \pi - \arcsin\left(\frac{\sqrt{3}}{2\sin(\gamma/2)}\right), \qquad \sigma_0^a(\gamma) := \arccos\left(\frac{\cos\gamma}{2}\right). \tag{28}$$

The notation corresponds to the fact that $\sigma_0^s = \lim_{\varepsilon\to 0}\sigma_\varepsilon^s$. Notice that $\gamma \mapsto \sigma_0^s(\gamma)$ is increasing on $[3\pi/4, \pi]$ and converging to $2\pi/3$ as $\gamma \uparrow \pi$. Thanks to (23) and (24) we also have that $\beta^s(\alpha,\gamma) > 2\pi/3$ if $\alpha < \sigma_0^s(\gamma)$. The definition of γ_ε^s and the monotonicity of $\sigma_\varepsilon^s(\gamma)$ entail that $\sigma_0^s(\gamma) > 2\pi/3 - \varepsilon$ for any $\varepsilon \in (0, \pi/8)$, as soon as $\gamma > \gamma_\varepsilon^s$.

We can now proceed with the optimization of $\mathcal{E}^s(\cdot,\gamma)$ as follows.

LEMMA 4.1 (minimality in α). *Given $\gamma \in (\gamma_\varepsilon^s, \pi)$, the map $\alpha \mapsto \mathcal{E}^s(\alpha,\gamma)$ admits a unique minimizer $\alpha^s(\gamma)$ on $(2\pi/3-\varepsilon, \sigma_\varepsilon^s(\gamma))$. Moreover, one has that $\alpha^s(\gamma) < 2\pi/3$, $\beta^s(\alpha^s(\gamma),\gamma) < 2\pi/3$, $\partial^2_{\alpha\alpha}\mathcal{E}^s(\alpha^s(\gamma),\gamma) > 0$, and $\alpha^s(\gamma) \to 2\pi/3$ as $\gamma \uparrow \pi$.*

Proof. Let $\gamma \in (\gamma_\varepsilon^s, \pi)$ be fixed. This ensures that $\sigma_\varepsilon^s(\gamma) > 2\pi/3$, by the definition of γ_ε^s.

First, we show that α is not a minimizer of $\alpha \mapsto \mathcal{E}^s(\alpha,\gamma)$ if $\beta^s(\alpha,\gamma) > 2\pi/3$. We recall that $\sigma_0^s(\gamma)$ is defined as the unique value in $(\pi/2, 2\pi/3)$ such that $\beta^s(\sigma_0^s(\gamma),\gamma) = 2\pi/3$ and that $\sigma_0^s(\gamma) > 2\pi/3 - \varepsilon$. If $\beta^s(\alpha,\gamma) > 2\pi/3$, the monotonicity of β^s from (23) and (24) shows that $2\pi/3 - \varepsilon < \alpha < \sigma_0^s(\gamma)$, and then we have

$$\begin{aligned}\mathcal{E}^s(\alpha,\gamma) &= 2v_3(\alpha) + v_3(\beta^s(\alpha,\gamma)) > 2v_3(\sigma_0^s(\gamma))\\ &= 2v_3(\sigma_0^s(\gamma)) + v_3(\beta^s(\sigma_0^s(\gamma),\gamma)) = \mathcal{E}_i(\sigma_0^s(\gamma),\gamma),\end{aligned}$$

where we have used the nonnegativity and the strict monotonicity of v_3 and the fact that $v_3(2\pi/3) = 0$.

One can similarly prove that there is no minimizer in $(2\pi/3, \sigma_\varepsilon^s(\gamma))$. Indeed, for α in such interval we have $\beta^s(\alpha,\gamma) \in I_\varepsilon$, from the obvious geometric constraint $2\alpha + \beta_i(\alpha,\gamma) < 2\pi$ and from the definition of $\sigma_\varepsilon^s(\gamma)$. Then, the monotonicity of $\alpha \mapsto \beta^s(\alpha,\gamma)$ and v_3 entails

$$\mathcal{E}^s(\alpha,\gamma) = 2v_3(\alpha) + v_3(\beta^s(\alpha,\gamma)) > v_3(\beta^s(2\pi/3,\gamma)) = \mathcal{E}^s(2\pi/3,\gamma).$$

Let now $\alpha \in (\sigma_0^s(\gamma), 2\pi/3)$. Then, we have just shown that $\beta^s(\alpha,\gamma) \in I_\varepsilon$. Since the composition of v_3 (convex and strictly decreasing on I_ε) and $\beta^s(\cdot,\gamma)$ (strictly concave) is strictly convex, it follows that $\mathcal{E}^s(\cdot,\gamma)$ is strictly convex in $(\sigma_0^s(\gamma), 2\pi/3)$. Let us now check that $\alpha \mapsto \mathcal{E}^s(\alpha,\gamma)$ is not minimized at the extrema $\sigma_0^s(\gamma)$ and $2\pi/3$, and this will conclude the proof. Since $\sigma_0^s(\gamma) > 2\pi/3 - \varepsilon$, we get

$$\partial_\alpha\mathcal{E}^s(\sigma_0^s(\gamma),\gamma) = 2v_3'(\sigma_0^s(\gamma)) + v_3'(\beta^s(\sigma_0^s(\gamma),\gamma))\partial_\alpha\beta^s(\sigma_0^s(\gamma),\gamma) = 2v_3'(\sigma_0^s(\gamma)) < 0,$$

because $v_3'(2\pi/3) = 0$ by assumption. Concerning $2\pi/3$, since $\beta^s(2\pi/3,\gamma) < 2\pi/3$, we have

$$\partial_\alpha\mathcal{E}^s(2\pi/3,\gamma) = 2v_3'(2\pi/3) + v_3'(\beta^s(2\pi/3,\gamma))\partial_\alpha\beta^s(2\pi/3,\gamma) > 0,$$

thanks once more to the monotonicity of v_3 and $\beta^s(\cdot,\gamma)$. The claim is proved, and the unique minimizer $\alpha^s(\gamma)$ belongs to $(\sigma_0^s(\gamma), 2\pi/3) \subset I_\varepsilon$.

Eventually, we have $\beta^s(\sigma_0^s(\gamma),\gamma) < 2\pi/3$ since $\alpha^s(\gamma) > \sigma_0^s(\gamma)$. It is clear from (27) that $\sigma_0^s(\gamma)$ tends to $2\pi/3$ as $\gamma \uparrow \pi$, so that $\alpha^s(\gamma)$ tends to $2\pi/3$ as well. ∎

Note that Lemma 4.1 generalizes [30, Thms. 4.3 and 6.1] to the case $\gamma \neq \gamma_\ell$.

We now turn to prove convexity. The following functions *angle energies* $\tilde{E}^s$ will be used:

$$\tilde{E}^z\left(\alpha^1,\alpha^2,\gamma\right) := v_3\left(\alpha^1\right) + v_3\left(\alpha^2\right) + v_3\left(\tilde{\beta}^s\left(\alpha^1,\alpha^2,\gamma\right)\right).$$

LEMMA 4.2 (convexity in α). *There exist $\check{\gamma}_\varepsilon^s \in (\gamma_\varepsilon^s, \pi)$ such that, for all $\gamma \in (\check{\gamma}_\varepsilon^s, \pi)$, the map $(\alpha^1,\alpha^2) \mapsto \tilde{E}^s(\alpha^1,\alpha^2,\gamma)$ is strictly convex on $[\sigma_0^s(\gamma), 2\pi/3] \times [\sigma_0^s(\gamma), 2\pi/3]$.*

Proof. Let $\gamma > \gamma_\varepsilon^s$ so that we have both $\sigma_\varepsilon^s(\gamma) > 2\pi/3$ and $\sigma_0^s(\gamma) > 2\pi/3 - \varepsilon$, as previously observed; see (27)–(28). By taking (23) and (24) into account we have that $\alpha \geq \sigma_0^s(\gamma) > 2\pi/3 - \varepsilon$ implies $\beta^s(\alpha,\gamma) \leq 2\pi/3$, and $\alpha \leq 2\pi/3 < \sigma_\varepsilon^s(\gamma)$ implies $\beta^s(\alpha,\gamma) > 2\pi/3 - \varepsilon$. Thanks to the monotonicity in (22), analogous bounds are found for $\tilde{\beta}^s$ as well. That is, if $\alpha^1,\alpha^2 \in [\sigma_0^s(\gamma), 2\pi/3] \subset I_\varepsilon$, then $\tilde{\beta}^s(\alpha^1,\alpha^2,\gamma) \in (2\pi/3 - \varepsilon, 2\pi/3] = I_\varepsilon$.

In the following ∇ denotes the derivative with respect to (α^1,α^2). The index s as well as the dependence of $\tilde{\beta}^s$ and $\tilde{E}^s$ on the three variables $(\alpha^1,\alpha^2,\gamma)$ will be omitted for brevity. For $\alpha^1,\alpha^2 \in [\sigma_0^s(\gamma), 2\pi/3]$, we have

$$\nabla^2\tilde{E}\left(\alpha^1,\alpha^2,\gamma\right) = \operatorname{diag}\left(v_3''\left(\alpha^1\right), v_3''\left(\alpha^2\right)\right) + v_3''(\tilde{\beta})\nabla\tilde{\beta}\otimes\nabla\tilde{\beta} + v_3'(\tilde{\beta})\nabla^2\tilde{\beta}.$$

A direct computation yields

$$\begin{aligned}
\tilde{E}_{\alpha^1\alpha^1}\left(\alpha^1,\alpha^2,\gamma\right) &= v_3''\left(\alpha^1\right) + \tilde{\beta}_{\alpha^1\alpha^1}v_3'(\tilde{\beta}) + \tilde{\beta}_{\alpha^1}^2 v_3''(\tilde{\beta}),\\
\tilde{E}_{\alpha^2\alpha^2}\left(\alpha^1,\alpha^2,\gamma\right) &= v_3''\left(\alpha^2\right) + \tilde{\beta}_{\alpha^2\alpha^2}v_3'(\tilde{\beta}) + \tilde{\beta}_{\alpha^2}^2 v_3''(\tilde{\beta}),\\
\tilde{E}_{\alpha^1\alpha^2}\left(\alpha^1,\alpha^2,\gamma\right) &= \tilde{\beta}_{\alpha^1\alpha^2}^2 v_3'(\tilde{\beta}) + \tilde{\beta}_{\alpha^1}\tilde{\beta}_{\alpha^2}v_3''(\tilde{\beta}),\\
\det\nabla^2\tilde{E} &= \left[v_3''\left(\alpha^1\right) + \beta_{\alpha^1\alpha^1}v_3'(\tilde{\beta})\right]\left[v_3''\left(\alpha^2\right) + \tilde{\beta}_{\alpha^2\alpha^2}v_3'(\tilde{\beta})\right]\\
&\quad + v_3''\left(\alpha^1\right)v_3''(\tilde{\beta})\tilde{\beta}_{\alpha^2}^2 + v_3''\left(\alpha^2\right)v_3''(\tilde{\beta})\tilde{\beta}_{\alpha^1}^2 - v_3'^2(\tilde{\beta})\tilde{\beta}_{\alpha^1\alpha^2}^2\\
&\quad - 2v_3'(\tilde{\beta})v_3''(\tilde{\beta})\tilde{\beta}_{\alpha^1}\tilde{\beta}_{\alpha^2}\tilde{\beta}_{\alpha^1\alpha^2},
\end{aligned}$$

where we have exploited the regularity of v_3; see section 2. In particular, we have $v_3'(2\pi/3) = 0$ and $v_3''(2\pi/3) > 0$. We recall that the functions $\tilde{\beta}^s(\alpha^1,\alpha^2,\gamma)$ are smooth and tend to $2\pi/3$ as $(\alpha^1,\alpha^2,\gamma)$ tends to $(2\pi/3, 2\pi/3, \pi)$; see (8). On the other hand, $\sigma_0^s(\gamma) \uparrow 2\pi/3$ as $\gamma \uparrow \pi$; see (28). Therefore, we can choose $\check{\gamma}_\varepsilon^s \in (\gamma_\varepsilon^s, \pi)$ such that, for all $(\alpha^1,\alpha^2) \in [\sigma_0^s(\gamma), 2\pi/3] \times [\sigma_0^s(\gamma), 2\pi/3]$ and $\gamma \in (\check{\gamma}_\varepsilon^s, \pi)$; it holds that

$$v_3''\left(\alpha^1\right) > \frac{1}{2}v_3''(2\pi/3), \qquad v_3''\left(\alpha^2\right) > \frac{1}{2}v_3''(2\pi/3), \qquad |\tilde{\beta}_{\alpha^1\alpha^1}v_3'(\tilde{\beta})| < \frac{1}{4}v_3''(2\pi/3)$$

and

$$\begin{aligned}
&\Big|v_3''\left(\alpha^1\right)\tilde{\beta}_{\alpha^2\alpha^2}v_3'(\tilde{\beta}) + v_3''\left(\alpha^2\right)\tilde{\beta}_{\alpha^1\alpha^1}v_3'(\tilde{\beta})\\
&\qquad + \left(\tilde{\beta}_{\alpha^1\alpha^1}\tilde{\beta}_{\alpha^2\alpha^2} - \tilde{\beta}_{\alpha^1\alpha^2}^2\right)v_3'^2(\tilde{\beta}) - 2v_3'(\tilde{\beta})v_3''(\tilde{\beta})\tilde{\beta}_{\alpha^1}\tilde{\beta}_{\alpha^2}\tilde{\beta}_{\alpha^1\alpha^2}\Big| < \frac{1}{8}(v_3''(2\pi/3))^2.
\end{aligned}$$

This way we get $4\tilde{E}_{\alpha^1\alpha^1} > v_3''(2\pi/3) > 0$ and $8\det\nabla^2\tilde{E} > (v_3''(2\pi/3))^2 > 0$ as desired. ∎

Let us now turn to analyze the dependence of $\mathcal{E}^s$ on γ. We have the following.

LEMMA 4.3 (monotonicity and convexity in γ). *There exists $\hat{\gamma}_\varepsilon^s \in (\gamma_\varepsilon^s, \pi)$ such that the map*

$$\gamma \mapsto \mathscr{E}^s(\gamma) := \mathcal{E}^s(\alpha^s(\gamma), \gamma) = \min\{\mathcal{E}^s(\alpha, \gamma) \mid \alpha \in (\sigma_0^s(\gamma), 2\pi/3)\}$$

is strictly decreasing and strictly convex on $(\hat{\gamma}_\varepsilon^s, \pi)$.

Proof. In the following, we drop the index s from β^s, $\mathcal{E}^s$, $\mathscr{E}^s$, γ_ε^s, $\hat{\gamma}_\varepsilon^s$, $\sigma_0^s(\gamma)$, and $\alpha^s(\gamma)$ for the sake of notational simplicity. Let $\gamma \in (\gamma_\varepsilon, \pi)$ and take derivatives with respect to γ. Thanks to first order optimality condition for $\alpha(\gamma)$, i.e., $\mathcal{E}_\alpha(\alpha(\gamma), \gamma) = 0$, we have

$$\mathscr{E}'(\gamma) = \mathcal{E}_\alpha(\alpha(\gamma), \gamma)\alpha'(\gamma) + \mathcal{E}_\gamma(\alpha(\gamma), \gamma) = v_3'(\beta(\alpha(\gamma), \gamma))\beta_\gamma(\alpha(\gamma), \gamma).$$

As $\beta(\alpha(\gamma), \gamma) < 2\pi/3$ from Proposition 4.1, we have $v_3'(\beta(\alpha(\gamma), \gamma)) < 0$ and we conclude from (23) and (24) that $\mathscr{E}' < 0$ on $(\gamma_\varepsilon, \pi)$. By taking the derivative with respect to γ in the identity $\mathcal{E}_\alpha(\alpha(\gamma), \gamma) = 0$, we get $\mathcal{E}_{\alpha\alpha}(\alpha(\gamma), \gamma)\alpha'(\gamma) + \mathcal{E}_{\alpha\gamma}(\alpha(\gamma), \gamma) = 0$, and thus

$$\alpha'(\gamma) = -\frac{\mathcal{E}_{\alpha\gamma}(\alpha(\gamma), \gamma)}{\mathcal{E}_{\alpha\alpha}(\alpha(\gamma), \gamma)}.$$

Using the latter expression for $\alpha'(\gamma)$, we find (here ∇ denotes derivation in the couple α, γ)

$$\begin{aligned}
\mathscr{E}''(\gamma) &= \mathcal{E}_{\alpha\gamma}(\alpha(\gamma), \gamma)\alpha'(\gamma) + \mathcal{E}_{\gamma\gamma}(\alpha(\gamma), \gamma) \\
&= \frac{\mathcal{E}_{\alpha\alpha}(\alpha(\gamma), \gamma)\mathcal{E}_{\gamma\gamma}(\alpha(\gamma), \gamma) - \mathcal{E}_{\alpha\gamma}^2(\alpha(\gamma), \gamma)}{\mathcal{E}_{\alpha\alpha}(\alpha(\gamma), \gamma)} \\
&= \frac{\det \nabla^2 \mathcal{E}(\alpha(\gamma), \gamma)}{\mathcal{E}_{\alpha\alpha}(\alpha(\gamma), \gamma)}.
\end{aligned}$$

The second-order optimality condition for $\alpha(\gamma)$ reads $\mathcal{E}_{\alpha\alpha}(\alpha(\gamma), \gamma) > 0$, as seen in Proposition 4.1. In order to check the positivity of $\mathscr{E}''$, we need to prove that $\det \nabla^2 \mathcal{E}(\alpha(\gamma), \gamma) > 0$. We check this property in a left neighborhood of $\gamma = \pi$. To this aim we compute the general expression of $\det \nabla^2 \mathcal{E}(\alpha, \gamma)$ on $(\sigma(\gamma), 2\pi/3) \times (\gamma_\varepsilon, \pi)$. The computations of second-order derivatives are similar to the ones in Lemma 4.2. We have that

$$\begin{aligned}
\mathcal{E}_{\alpha\alpha} &= 2v_3''(\alpha) + \beta_\alpha^2 v_3''(\beta) + \beta_{\alpha\alpha} v_3'(\beta), \\
\mathcal{E}_{\gamma\gamma} &= \beta_\gamma^2 v_3''(\beta) + \beta_{\gamma\gamma} v_3'(\beta), \\
\mathcal{E}_{\alpha\gamma} &= \beta_\alpha \beta_\gamma v_3''(\beta) + \beta_{\alpha_\gamma} v_3'(\beta).
\end{aligned}$$

These entail in particular that

$$\begin{aligned}
\det \nabla^2 \mathcal{E} = {} & 2v_3''(\alpha)v_3''(\beta)\beta_\gamma^2 + 2v_3''(\alpha)v_3'(\beta)\beta_{\gamma\gamma} \\
& + v_3'(\beta)v_3''(\beta)\left(\beta_\alpha^2\beta_{\gamma\gamma} + \beta_\gamma^2\beta_{\alpha\alpha} - 2\beta_\alpha\beta_\gamma\beta_{\alpha\gamma}\right) \\
& + v_3'^2(\beta)\left(\beta_{\alpha\alpha}\beta_{\gamma\gamma} - \beta_{\alpha\gamma}^2\right).
\end{aligned}$$

Recall now from Proposition 4.1 that if $\gamma \uparrow \pi$ we also have $\alpha(\gamma) \to 2\pi/3$, and then

$\beta(\alpha(\gamma),\gamma) \to 2\pi/3$ as well. Taking (25)–(26) into account, one finds that $\beta_\gamma^2\beta_{\alpha\alpha} - 2\beta_\alpha\beta_\gamma\beta_{\alpha\gamma}$ is negligible with respect to $\beta_\alpha^2\beta_{\gamma\gamma}$, which has a nonzero limit as $\gamma \uparrow \pi$, and that the term involving $\beta_\alpha^2\beta_{\gamma\gamma}$ dominates the ones involving $v_3'^2(\beta)$. Indeed, we have $\beta \to 2\pi/3$ and $|v_3'^2(\beta)| \ll v_3'(\beta)v_3''(\beta)$, since $v_3'(2\pi/3) = 0$ and $v_3''(2\pi/3) > 0$. Therefore, there exists $\hat\gamma_\varepsilon \in (\gamma_\varepsilon, \pi)$ such that the sign of $\det \nabla^2\mathcal{E}(\alpha(\gamma),\gamma)$ in $(\hat\gamma_\varepsilon,\pi)$ is the same as that of

$$
\begin{aligned}
&2v_3''(\alpha(\gamma))v_3''(\beta(\alpha(\gamma),\gamma))\beta_\gamma^2(\alpha(\gamma),\gamma)\\
&\quad + 2v_3''(\alpha(\gamma))v_3'(\beta(\alpha(\gamma),\gamma))\beta_{\gamma\gamma}(\alpha(\gamma),\gamma)\\
&\quad + v_3'(\beta(\alpha(\gamma),\gamma))v_3''(\beta(\alpha(\gamma),\gamma))\beta_\alpha^2(\alpha(\gamma),\gamma)\beta_{\gamma\gamma}(\alpha(\gamma),\gamma).
\end{aligned}
$$

The latter is positive thanks to (23)–(24) and the fact that $v_3'(\beta(\alpha(\gamma),\gamma)) < 0$ because of $\beta(\alpha(\gamma),\gamma) < 2\pi/3$. ∎

Moving from Lemma 4.1 one can prove that the configurational energy E admits a unique minimizer on the family $\mathscr{F}_\ell^s$, recovering indeed [30, Thms. 4.3 and 6.1]. In fact, by (14) and (21) such minimization reduces to the minimization of the angle energy of a single point, namely,

$$
\min\left\{\mathcal{E}^s(\alpha,\gamma_\ell) : \alpha \in (2\pi/3-\varepsilon, \sigma_\varepsilon^s(\gamma_\ell))\right\}. \tag{29}
$$

In fact, following section 3 we should require $\alpha \in (\alpha_-^s, \alpha_+^s)$ from (11)–(12) and (18)–(19). Note nonetheless that

$$
(2\pi/3-\varepsilon, \sigma_\varepsilon^s(\gamma_\ell)) \subset (\alpha_-^s, \alpha_+^s)
$$

if $v_2(r) = 0$ for $r \geq 1.1$ and $\ell \geq 4$ in the zigzag case or $\ell \geq 6$ in the armchair case. Lemma 4.1 entails the following.

THEOREM 4.4 (minimality in $\mathscr{F}_\ell^s$). *Letting $\ell \geq 4$ (zigzag) or $\ell \geq 6$ (armchair), there exists a unique nanotube $\mathcal{F}_\ell^s \in \mathscr{F}_\ell^s$ minimizing E within $\mathscr{F}_\ell^s$. This corresponds to the unique minimizer of $\alpha \mapsto \mathcal{E}^s(\alpha,\gamma_\ell)$ in $(2\pi/3-\varepsilon, \sigma_\varepsilon^s(\gamma_\ell))$.*

Before closing this section, let us mention again that the minimizing nanotubes $\mathcal{F}_\ell^s$ do not coincide with the rolled-up [10] nor with the polyhedral nanotubes [6]. Indeed, these are defined via their corresponding angles $\alpha_{\rm ru}^s = 2\pi/3$ and by $\alpha_{\rm poly}^s$ solving $\beta^s(\alpha_{\rm poly}^s,\gamma_\ell) = \alpha_{\rm poly}^s$. One easily checks that $\partial_\alpha\mathcal{E}^s(\cdot,\gamma_\ell) \neq 0$ both in $\alpha_{\rm ru}^s$ and $\alpha_{\rm poly}^s$; see [30, Thms. 4.1–4.2 and 6.1].

5. Proof of Theorem 2.1. We are eventually in the position of proving the assertion of Theorem 2.1.

Define ℓ_ε^s as the smallest integer (larger than 2) such that

$$
\gamma_{\ell_\varepsilon^s} > \max\{\tilde\gamma_\varepsilon^s, \hat\gamma_\varepsilon^s\},
$$

where $\tilde\gamma_\varepsilon^s$ and $\hat\gamma_\varepsilon^s$ appear in Lemmas 4.2 and 4.3. Notice from the proofs of such lemmas

that the numbers $\check{\gamma}^s_\varepsilon$ and $\hat{\gamma}^s_\varepsilon$ are depending on the specific choice of the potential v_3. Fix the integer $\ell > \ell^s_\varepsilon$ from now on. Let moreover η^s_ε be the largest positive number such that

(i) the n-cell $\{x_1, \dots, x_n\}$ of any nanotube in $\mathscr{P}_{\eta^s_\varepsilon}(\mathcal{F}^s_\ell)$ satisfies (3), and moreover
(ii) the angle γ^s_i at x_i satisfies $\gamma^s_i > \max\{\check{\gamma}^s_\varepsilon, \hat{\gamma}^s_\varepsilon\}$, and the angles α^1_i, α^2_i at x_i belong to $(\sigma^s_0(\gamma^s_i), 2\pi/3)$ for any $i = 1, \dots, n$.

The number η^s_ε gives the smallness of the perturbation and depends on v_3, ε, and on ℓ.

Let now $\mathcal{F}^s_\ell \in \mathscr{F}^s_\ell$ be the minimal nanotube from Theorem 4.4 and $\tilde{\mathcal{F}} \in \mathscr{P}_{\eta^s_\varepsilon}(\mathcal{F}^s_\ell)$ be a nontrivial perturbation with n-cell $\{x_1, \dots, x_n\}$. In particular, the restrictions on ℓ and η^s_ε entail that the topology of $\mathcal{F}^s_\ell$ and that of $\tilde{\mathcal{F}}$ coincide and the energy $E(\tilde{\mathcal{F}})$ can be computed as

$$E(\tilde{\mathcal{F}}) = E(F_n, L) = \frac{1}{2}\sum_{i=1}^{n}\sum_{k=1}^{3} v_2(|x_i - x_{i_k}|_L) + \sum_{i=1}^{n} \tilde{E}^s\left(\alpha^1_i, \alpha^2_i, \gamma^s_i\right),$$

where x_{i_k}, $k = 1, 2, 3$, are the three points that are bonded to x_i. We recall that $\overline{\gamma}$ is given by (4) and that we are assuming $\bar{\gamma} \le \gamma_\ell$. As $v_2 \ge -1$, we get the bound

$$E(\tilde{\mathcal{F}}) \ge -\frac{3}{2}\, n + \sum_{i=1}^{n} \tilde{E}^s\left(\alpha^1_i, \alpha^2_i, \gamma^s_i\right).$$

By letting $\alpha_i := (\alpha^1_i + \alpha^2_i)/2$ we have

$$\sum_{i=1}^{n} \tilde{E}^s\left(\alpha^1_i, \alpha^2_i, \gamma^s_i\right) \ge \sum_{i=1}^{n} \mathcal{E}^s(\alpha_i, \gamma^s_i) \ge \sum_{i=1}^{n} \mathcal{E}^s(\alpha_i(\gamma^s_i), \gamma^s_i) = \sum_{i=1}^{n} \mathscr{E}^s(\gamma^s_i) \ge n\mathscr{E}^s(\overline{\gamma}),$$

where we have used Lemma 4.2, the definition of $\alpha^s(\gamma^s_i)$ as the unique minimizer of $\alpha \mapsto \mathcal{E}^s(\alpha, \gamma^s_i)$ from Lemma 4.1, and the definition of $\mathscr{E}^s$ and its convexity from Lemma 4.3. (Note that all the angles γ^s_i, α^1_i, and α^2_i belong to the correct range of validity of these properties thanks to the restrictions on ℓ and η^s_ε.) We have obtained

$$E(\tilde{\mathcal{F}}) \ge -3n/2 + n\mathscr{E}^s(\overline{\gamma}).$$

As $\mathscr{E}^s$ is decreasing due to Lemma 4.3, from the assumption $\overline{\gamma} \le \gamma_\ell$ we deduce that

$$E(\tilde{\mathcal{F}}) \ge -3n/2 + n\mathscr{E}_i(\gamma_\ell) = E(\mathcal{F}^s_\ell).$$

The assertion follows upon noting that equality holds if and only if the perturbation is trivial, since all the convexity and monotonicity properties we used are strict. Note that the proof is independent from the period L of $\tilde{\mathcal{F}}$, which is a small perturbation of the one of $\mathcal{F}^s_\ell$.

6. Numerical evidence for (5). Theorem 2.1 asserts the stability of $\mathcal{F}^s_\ell$ with respect to all small perturbations fulfilling $\overline{\gamma} \le \gamma_\ell$. Under assumption (5) the reach of the result could then be readily extended to all small perturbations. As we are presently not able to present an analytical proof of (5), we resort to recording here some numerical evidence under the specific choice of v_2 and v_3 given for $f(t) := 1/(2t^{12}) - 1/t^6$ by

$$v_2(r) = \begin{cases} f(r) - f(1.1) & \text{if } 0 < r < 1.1, \\ 0 & \text{otherwise,} \end{cases} \qquad v_3(\theta) = 10(\cos\theta + 1/2)^2.$$

These interaction potentials fulfill the general requirements of section 2. In particular, v_2 is a short-ranged, truncated version of the classical Lennard-Jones potential and v_3 corresponds to the standard choice in [42]. We argue on the zigzag and the armchair case separately.

Zigzag. Fix $\ell \in \mathbb{N}$ suitably large and let $\mathcal{F}^z_\ell = (F^z_n, L^z_n)$ be the optimal configuration in $\mathscr{F}^z_\ell$. Recall hat the n-cell F^z_n is characterized by $\alpha^z(\gamma_\ell)$, which is the unique minimum in (29). The reference period is the cell length $L^z_n := 2m(1 - \cos\alpha^z(\gamma_\ell))$, where the integers m, n, ℓ are such that $n = 4m\ell$; see (13). As usual, e_3 is the axis of the nanotube.

Now let $\widetilde{\mathcal{F}} := (F_n, L)$ be a small perturbation of $\mathcal{F}^z_\ell$. Notice that, as in the definition of $\mathscr{P}_{\eta^s_\varepsilon}(\mathcal{F}^s_\ell)$ in section 2, we are perturbing the position of the points in the n-cell F^z_n *and* the period L^z_n. For every point x in F_n, let x_1, x_2, x_3 be the points that are bonded to x (modulo L). We define the new configuration $\overline{\mathcal{F}} := (\overline{F}_n, L)$ by letting its n-cell $\overline{F}_n$ be obtained by rigidly rotating around the midpoint each bond in $\widetilde{\mathcal{F}}$ corresponding to a bond in $\mathcal{F}^s_n$ parallel to e_3, in such a way that the rotated bond is again parallel to e_3.

A comparison between the energies $E(\widetilde{\mathcal{F}})$ and $E(\overline{\mathcal{F}})$ is given in Figure 6 with respect to two different reference configurations, namely, $\ell = 10$, $m = 2$ ($n = 80$) in the top and $\ell = 20$, $m = 2$ ($n = 160$) in the bottom subfigure. We ran the comparison over 10^6 random perturbations $\widetilde{\mathcal{F}}$, 10^2 of which are plotted in Figure 6. The horizontal axis of the diagram is the mean $\overline{\gamma}$ of the angles γ^z_i, whereas the vertical axis corresponds to the energy (normalized with respect to the number n of atoms). Each random perturbation $\widetilde{\mathcal{F}}$ is denoted by a cross in the diagram and is linked via a dotted line to its corresponding configuration $\overline{\mathcal{F}}$, indicated by a circle. The decrease of the energy $E(\widetilde{\mathcal{F}}) \ge E(\overline{\mathcal{F}})$ as well as the fact that $\overline{\gamma} = \gamma_\ell$ for $\overline{\mathcal{F}}$ are apparent, so that (5) is confirmed.

The experiment gives also an illustration of Theorem 2.1, for all random perturbations have a higher energy when compared to the optimal configuration $\mathcal{F}^z_\ell$.

Armchair. We start from the optimal configuration $\mathcal{F}^a_\ell = (F^a_n, L^a_n)$ corresponding indeed to the unique angle $\alpha^a(\gamma_\ell)$ realizing the minimum in (29). The period L^a_n is given by (20) for suitable integers n, m, ℓ with ℓ even and $n = 2m\ell$.

Assume to be given a small perturbation $\widetilde{\mathcal{F}} = (F_n, L)$ of $\mathcal{F}^a_\ell$. Let us indicate by b_{ik} the bond corresponding to that of $\mathcal{F}^a_\ell$ with endpoints indexed as $(i, 0, k)$ and $(i, 1, k)$ in (15). We define $\overline{\mathcal{F}}$ fulfilling (5) by $\overline{\mathcal{F}} = T(\widetilde{\mathcal{F}})$, where the transformation T is the composition of some elementary transformations T_i for $i = 0, \dots, 3$ defined as follows.

T_0: Rotate each b_{ik} around its midpoint in such a way that the rotated bond lays in an orthogonal plane to e_3 and its endpoints are equidistant from e_3.

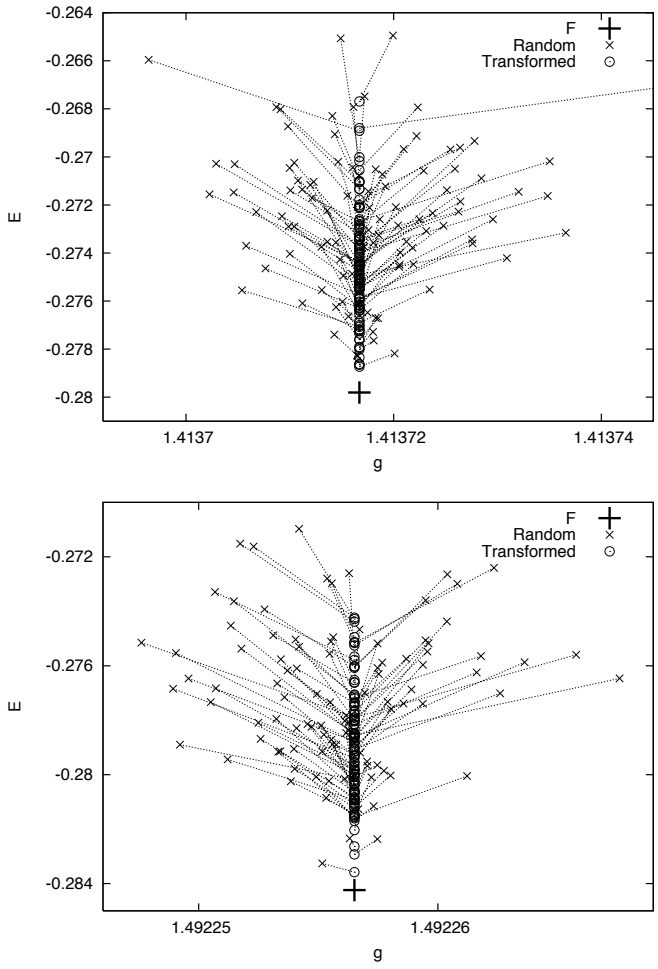

FIG. 6. *Comparison of the energy of a random perturbation $\widetilde{\mathcal{F}}$ of $\mathcal{F}_\ell^z$ with the energy of its corresponding configuration $\overline{\mathcal{F}}$. We have investigated the two cases $\ell = 10$, $n = 80$ (above) and $\ell = 20$, $n = 160$ (below). Energy values (normalized with respect to n) are on the vertical axis, while the horizontal axis depicts the mean angle $\overline{\gamma}$ of each configuration. The energy of each random perturbation $\widetilde{\mathcal{F}}$ (cross) is higher than the energy of its corresponding configuration $\overline{\mathcal{F}}$ (circle), which satisfies $\overline{\gamma} = \gamma_\ell$. The cross at the bottom corresponds to the minimizer $\mathcal{F}_\ell^z$.*

T_1: Rotate each b_{ik} around its midpoint first and then around e_3 in such a way that the rotated bond is parallel to the corresponding bond in $\mathcal{F}_\ell^a$ and its endpoints are equidistant from e_3.

T_2: For each i compute the mean d_i of the distances of the midpoints of the bonds b_{ik} to e_3. Translate each b_{ik} by displacing its midpoint in the radial direction with respect to e_3 in such a way that the distance of the displaced midpoint from e_3 is exactly d_i.

T_3: For each i compute the mean s_i of lengths of the bonds b_{ik}. Dilate/contract each b_{ik} about its midpoint without rotating it so that the transformed bond has length s_i.

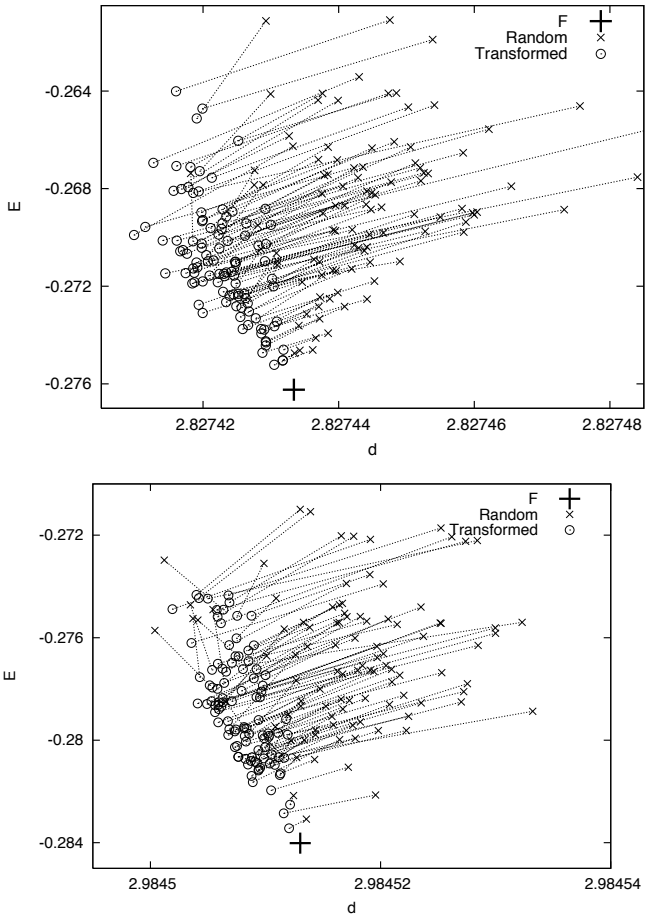

FIG. 7. *Comparison of the energy of a random perturbation* $\widetilde{\mathcal{F}}$ *of* $\mathcal{F}_\ell^a$ *with the energy of its transformed configuration* $T_2(T_0(\widetilde{\mathcal{F}}))$. *We investigate the two cases* $\ell = 10$, $n = 80$ *(above) and* $\ell = 20$, $n = 160$ *(below). Energy values (normalized with respect to* n*) are on the vertical axis, while the horizontal axis depicts the mean angle* $\overline{\gamma}$ *of each configuration. The energy of each random perturbation* $\widetilde{\mathcal{F}}$ *(cross) is higher than the energy of its transformed configuration* $T_2(T_0(\widetilde{\mathcal{F}}))$ *(circle), which satisfies* $\overline{\gamma} \le \gamma_\ell$. *The cross at the bottom corresponds to the minimizer* $\mathcal{F}_\ell^a$.

Figures 7 and 8 show random perturbations $\widetilde{\mathcal{F}}$ (crosses) and the transformed configurations $\overline{\mathcal{F}} = T(\widetilde{\mathcal{F}})$ (circles) corresponding to the choices $T = T_2 \circ T_0$ (Figure 7) and $T = T_3 \circ T_2 \circ T_1$ (Figure 8) and the two reference choices for the n-cell $\ell = 10$, $m = 4$, $n = 80$ (top), and $\ell = 20$, $m = 4$, $n = 160$ (bottom). Normalized energies with respect to the number of atoms and mean $\overline{\gamma}$ of the angles γ_i^a are depicted on the vertical and on the horizontal axis, respectively. We have run the simulation over 10^6 random perturbation, of which 10^2 are reported here.

In the case $T = T_2 \circ T_0$ (Figure 7), we have that $E(\overline{\mathcal{F}}) \le E(\widetilde{\mathcal{F}})$ and that the mean angle $\overline{\gamma}$ of $\overline{\mathcal{F}}$ becomes smaller than γ_ℓ. In the case $T = T_3 \circ T_2 \circ T_1$ (Figure 8), we have that $E(\overline{\mathcal{F}}) \le E(\widetilde{\mathcal{F}})$ and $\overline{\gamma} = \gamma_\ell$. This last equality could also be proved by means of direct geometric considerations from the definitions of the transformations. In both cases (5) holds.

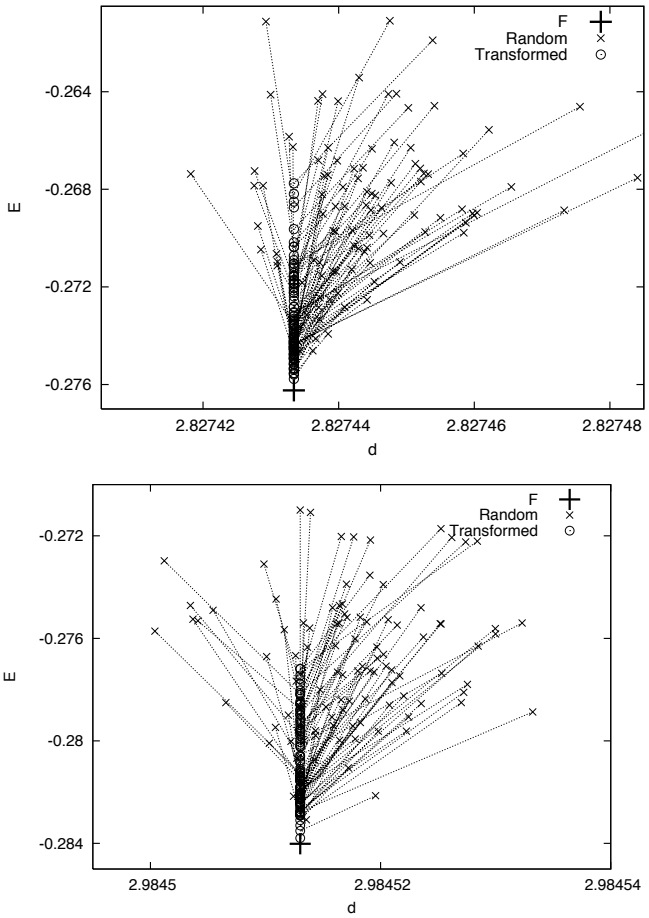

FIG. 8. *Comparison of the energy of a random perturbation* $\widetilde{\mathcal{F}}$ *of* $\mathcal{F}_\ell^a$ *with the energy of its transformed configuration* $T_3(T_2(T_1(\widetilde{\mathcal{F}})))$. *We investigate the two cases* $\ell = 10$, $n = 80$ *(above) and* $\ell = 20$, $n = 160$ *(below). Energy values (normalized with respect to* n*) are on the vertical axis, while the horizontal axis depicts the mean angle* $\overline{\gamma}$ *of each configuration. The energy of each random perturbation* $\widetilde{\mathcal{F}}$ *(cross) is higher than the energy of its transformed configuration* $T_3(T_2(T_1(\widetilde{\mathcal{F}})))$ *(circle), which satisfies* $\overline{\gamma} = \gamma_\ell$. *The cross at the bottom corresponds to the minimizer* $\mathcal{F}_\ell^a$.

Note that all perturbations have higher energy with respect to $\mathcal{F}_\ell^a$.

Acknowledgment. The authors would like to acknowledge the kind hospitality of the Erwin Schrödinger International Institute for Mathematics and Physics, where part of this research was developed under the frame of the thematic program *Nonlinear Flows*.

REFERENCES

[1] N. L. ALLINGER, *Molecular Structure: Understanding Steric and Electronic Effects from Molecular Mechanics*, Wiley, New York, 2010.

[2] D. S. BETHUNE, C. H. KIANG, M. S. DE VRIES, G. GORMAN, R. SAVOY, ET AL., *Cobalt catalysed growth of carbon nanotubes with single-atomic-layer walls*, Nature, 363 (1993), pp. 605–607.

[3] B. R. Brook, R. E. Bruccoleri, B. D. Olafson, D. J. States, S. Swaminathan, and M. Karplus, *CHARMM: A program for macromolecular energy, minimization, and dynamics calculations*, J. Comput. Chem., 4 (1983), pp. 187–217
[4] J. Clayden, N. Greeves, and S. G. Warren, *Organic Chemistry*, Oxford University Press, Oxford, 2012.
[5] M. Clark, R. D. Cramer III, and N. Van Opdenbosch, *Validation of the general purpose tripos* 5.2 *force field*, J. Comput. Chem., 10 (1989), pp. 982–1012.
[6] B. J. Cox and J. M. Hill, *Exact and approximate geometric parameters for carbon nanotubes incorporating curvature*, Carbon, 45 (2007), pp. 1453–1462.
[7] B. J. Cox and J. M. Hill, *Geometric structure of ultra-small carbon nanotubes*, Carbon, 46 (2008), pp. 711–713.
[8] M. F. De Volder, S. H. Tawfick, R. H. Baughman, and A. J. Hart, *Carbon nanotubes: Present and future commercial applications*, Science, 339 (2013), pp. 535–539.
[9] M. S. Dresselhaus, G. Dresselhaus, and R. Saito, *Carbon fibers based on* C_{60} *ad their symmetry*, Phys. Rev. B, 45 (1992), pp. 6234–6242.
[10] M. S. Dresselhaus, G. Dresselhaus, and R. Saito, *Physics of Carbon Nanotubes*, Carbon, 33 (1995), pp. 883–891.
[11] W. E and D. Li, *On the crystallization of* $2D$ *hexagonal lattices*, Comm. Math. Phys., 286 (2009), pp. 1099–1140.
[12] W. E and P. Ming, *Cauchy–Born rule and the stability of crystalline solids: Static problems*, Arch. Ration. Mech. Anal., 183 (2007), pp. 241–297.
[13] D. El Kass and R. Monneau, *Atomic to continuum passage for nanotubes. A discrete Saint-Venant principle and error estimates*, Arch. Ration. Mech. Anal., 213 (2014), pp. 25–128.
[14] R. S. Elliott, N. Triantafyllidis, and J. A. Shaw, *Stability of crystalline solids*-I: *Continuum and atomic lattice considerations*, J. Mech. Phys. Solids, 54 (2006), pp. 161–192.
[15] R. S. Elliott, J. A. Shaw, and N. Triantafyllidis, *Stability of crystalline solids*-II: *Application to temperature-induced martensitic phase transformations in a bi-atomic crystal*, J. Mech. Phys. Solids, 54 (2006), pp. 193–232.
[16] B. Farmer. S. Esedoğlu, and P. Smereka, *Crystallization for a Brenner-like potential*, Comm. Math. Phys., 349 (2017), pp. 1029–1061.
[17] M. Friedrich, E. Mainini, P. Piovano, and U. Stefanelli, *Characterization of Optimal Carbon Nanotubes Under Stretching and Validation of the Cauchy–Born Rule*, arXiv:1706.01494, submitted, 2017.
[18] M. Friedrich, P. Piovano, and U. Stefanelli, *The geometry of* C_{60}*: A rigorous approach via Molecular Mechanics*, SIAM J. Appl. Math., 76 (2016), pp. 2009–2029.
[19] W. F. van Gunsteren and H. J. C. Berendsen, *Groningen Molecular Simulation (GROMOS) Library Manual*, BIOMOS b.v., Groningen, 1987.
[20] P. J. F. Harris, *Carbon Nanotube Science Synthesis, Properties and Applications*, Cambridge University Press, Cambridge, 2009.
[21] S. Iijima, *Helical microtubules of graphitic carbon*, Nature, 354 (1991), pp. 56–58.
[22] S. Ijima and T. Ichihashi, *Single-shell carbon nanotubes of* 1*-nm diameter*, Nature, 363 (1993), pp. 603–605.
[23] R. D. James, *Objective structures*, J. Mech. Phys. Solids, 54 (2006), pp. 2354–2390.
[24] A. Jorio, G. Dresselhaus, and M. S. Dresselhaus, eds., *Carbon nanotubes advanced topics in the synthesis, structure, properties and applications*, Topics in Applied Physics, Vol. 111. Springer, New York, 2011.
[25] K. Kanamits and S. Saito, *Geometries, electronic properties, and energetics of isolated single-walled carbon nanotubes*, J. Phys. Soc. Japan, 71 (2002), pp. 483–486.
[26] A. Krishnan, E. Dujardin, T. W. Ebbesen, P. N. Yianilos, and M. M. J. Treacy, *Young's modulus of single-walled nanotubes*, Phys. Rev. B, 58 (1998), pp. 14013–14019.
[27] R. K. F. Lee, B. J. Cox, and J. M. Hill, *General rolled-up and polyhedral models for carbon nanotubes*, Fullerenes, Nanotubes and Carbon Nanostructures, 19 (2011), pp. 726–748.
[28] E. G. Lewars, *Computational Chemistry*, 2nd ed., Springer, New York, 2011.
[29] E. Mainini and U. Stefanelli, *Crystallization in carbon nanostructures*, Comm. Math. Phys., 328 (2014), pp. 545–571.
[30] E. Mainini, H. Murakawa, P. Piovano, and U. Stefanelli, *Carbon-nanotube geometries: Analytical and numerical results*, Discrete Contin. Dyn. Syst. Ser. S, 10 (2017), pp. 141–160.
[31] S. L. Mayo, B. D. Olafson, and W. A. Goddard, *DREIDING: A generic force field for molecular simulations*, J. Phys. Chem., 94 (1990), pp. 8897–8909.
[32] M. Monthioux and V. L. Kuznetsov, *Who should be given the credit for the discovery of carbon nanotubes?*, Carbon, 44 (2006), pp. 1621–1623.

[33] T. W. Odom, J. L. Huang, P. Kim, and C. M. Lieber, *Atomic structure and electronic properties of single-walled carbon nanotubes*, Nature, 391 (1998), pp. 62–64.
[34] L. V. Radushkevich and V. M. Lukyanovich, *O strukture ugleroda, obrazujucegosja pri termiceskom razlozenii okisi ugleroda na zeleznom kontakte*, Zurn. Fisic. Chim., 26 (1952), pp. 88–95.
[35] A. K. Rappé and C. L. Casewit, *Molecular Mechanics Across Chemistry*, University Science Books, Sausalito, CA, 1997.
[36] D. Sfyris, *Phonon, Cauchy–Born and homogenized stability criteria for a free-standing monolayer graphene at the continuum level*, Eur. J. Mech. A Solids, 55 (2016), pp. 134–148.
[37] L. Shen and J. Li, *Transversely isotropic elastic properties of single-walled carbon nanotubes*, Phys. Rev. B, 69 (2004), 045414.
[38] L. Shen and J. Li, *Erratum: Transversely isotropic elastic properties of single-walled carbon nanotubes*, Phys. Rev. B, 81 (2010), 119902.
[39] L. Shen and J. Li, *Equilibrium structure and strain energy of single-walled carbon nanotubes*, Phys. Rev. B, 71 (2005), 165427.
[40] U. Stefanelli, *Stable carbon configurations*, Boll. Unione Mat. Ital. (9), 10 (2017), pp. 335–354.
[41] F. H. Stillinger and T. A. Weber, *Computer simulation of local order in condensed phases of silicon*, Phys. Rev. B, 8 (1985), pp. 5262–5271.
[42] J. Tersoff, *New empirical approach for the structure and energy of covalent systems*, Phys. Rev. B, 37 (1988), pp. 6991–7000.
[43] M. M. J. Treacy, T. W. Ebbesen, and J. M. Gibson, *Exceptionally high Young's modulus observed for individual carbon nanotubes*, Nature, 381 (1996), pp. 678–680.
[44] X. Wang, Q. Li, J. Xie, Z. Jin, J. Wang, Y. Li, K. Jiang, and S. Fan, *Shoushan. Fabrication of ultralong and electrically uniform single-walled carbon nanotubes on clean substrates*, Nano Lett., 9 (2009), pp. 3137–3141.
[45] P. K. Weiner and P. A. Kollman, *AMBER: Assisted model building with energy refinement. A general program for modeling molecules and their interactions*, J. Comput. Chem., 2 (1981), pp. 287–303.
[46] M.-F. Yu, B. S. Files, S. Arepalli, and R. S. Ruoff, *Tensile loading of ropes of single wall carbon nanotubes and their mechanical properties*, Phys. Rev. Lett., 84 (2000), pp. 5552–5555.
[47] T. Zhang, Z. S. Yuan, and L. H. Tan, *Exact geometric relationships, symmetry breaking and structural stability for single-walled carbon nanotubes*, Nano-Micro Lett., 3 (2011), pp. 28–235.